

References

¹ Elverum, G. W., Jr. and Staudhammer, P., "The Effect of Rapid Liquid-Phase Reactions on Injector Design and Combustion in Rocket Motors," Progress Rept. 30-4, Aug. 1959, Jet Propulsion Lab., Pasadena, Calif.

² Johnson, B. H., "An Experimental Investigation of the Effects of Combustion on the Mixing of Highly Reactive Liquid Propellants," TR 32-689, N65-33139, July 1965, Jet Propulsion Lab., Pasadena, Calif.

³ Stanford, H. B. and Tyler, W. H., "Injector Development," *Supporting Research and Advanced Development, JPL Space Programs Summary 37-51*, Vol. IV, Feb. 1965, Jet Propulsion Lab., Pasadena, Calif., p. 192.

⁴ Stanford, H. B., "Injector Development," *Supporting Research and Advanced Development, JPL Space Programs Summary 37-36*, N66-19041, Vol. IV, Dec. 1965, Jet Propulsion Lab., Pasadena, Calif., p. 174.

⁵ Riebling, R. W., "Injector Development: Impinging Sheet Injector," *Supporting Research and Advanced Development, JPL Space Programs Summary 37-45*, N67-34761, Vol. IV, June 1967, Jet Propulsion Lab., Pasadena, Calif.

⁶ Woodward, J. W., "Combustion Effects in Sprays," *Supporting Research and Advanced Development, JPL Space Programs Summary 37-36*, N66-19041, Vol. IV, Dec. 1965, Jet Propulsion Lab., Pasadena, Calif.

⁷ Burrows, M. C., "Mixing and Reaction of Hydrazine and Nitrogen Tetroxide at Elevated Pressure," *AIAA Journal*, Vol. 5, No. 9, Sept. 1967, pp. 1700-1701.

⁸ Lawver, B. R. and Breen, B. P., "Hypergolic Stream Impingement Phenomena-Nitrogen Tetroxide/Hydrazine," NAS-CR-7244, N68-37831, Oct. 1968, Dynamic Science Div., Marshall Industries, Monrovia, Calif.

⁹ Zung, L. B., "Hypergolic Impingement Mechanisms and Criteria for Jet Mixing or Separation," AD865675L, presented at the 6th ICRPG Liquid Propellant Combustion Instability Conference, Sept. 9-11, 1969, Dynamic Science Corp., Monrovia, Calif.

¹⁰ R-7223P, *Reactive Stream Impingement*, Rocketdyne, a Division of North American Rockwell Corp., Sept. 29, 1967.

¹¹ Houseman, J., "Jet Separation and Optimum Mixing for an Unlike Doublet," AD865675L, presented at the 6th ICRPG Liquid Propellant Combustion Instability Conference, Sept. 9-11, 1969, Jet Propulsion Lab., Pasadena, Calif.

¹² Kushida, R. and Houseman, J., "Criteria for Separation of Impinging Streams of Hypergolic Propellants," TM 33-395, N69-21082, July 1968, Jet Propulsion Lab., Pasadena, Calif.

¹³ Wuerker, R. F., Matthews, B. J., and Briones, R. A., "Producing Holograms of Reacting Sprays in Liquid Propellant Rocket Engines," Rept. 68.4712.2-024, N68-36737, July 31, 1968, TRW Systems Group, Redondo Beach, Calif.

¹⁴ H. Perlee, private communication, Dec. 12, 1969, Bureau of Mines, Bruceton, Pa.

¹⁵ Clayton, R. M., unpublished work, Oct. 1959, Jet Propulsion Lab., Pasadena, Calif.

¹⁶ Mills, T. R., Breen, B. P., and Lawver, B. R., "Transients Influencing Rocket Engine Ignition and Popping, Interim Report," Contract NAS7-467, N69-35533, CR-105315, April 30, 1969, Dynamic Science, Monrovia, Calif.

SEPTEMBER 1971

AIAA JOURNAL

VOL. 9, NO. 9

Spectral Infrared Reflectance of H_2O Condensed on LN_2 -Cooled Surfaces in Vacuum

B. E. WOOD,* A. M. SMITH,† J. A. ROUX,‡ AND B. A. SEIBER§
ARO, Inc., Arnold Air Force Station, Tenn.

Absolute hemispherical-angular reflectance measurements were made for H_2O cryodeposits formed in a vacuum infrared integrating sphere. These deposits were condensed on cryogenically cooled black epoxy paint and polished stainless steel surfaces at pressures between 2×10^{-2} and 4×10^{-2} torr. The results obtained are presented as functions of view angle from 0° to 60° , deposit thickness from 0 to 4.0 mm, and wavelength from 0.5 to 12.0μ . All three structural forms of ice I (hexagonal, cubic, and amorphous) were observed with the form occurring being a function of cryosurface temperature. The reflectance of any H_2O deposit was found to be strongly dependent on the form of ice present. From the results obtained in this investigation important conclusions are drawn with regard to effects on cooled optics and space simulation studies in ground test facilities.

Introduction

IN the fields of space simulation, radiative transfer, planetary environments, etc., there are numerous reasons for interest in the optical properties of ice, frost, or cryodeposit. For example, in space simulation testing of cryogenically

cooled detectors, the condensation of H_2O on cooled mirrors, windows, and lenses or on the test chamber cryowall can be undesirable as the condensate may alter the thermal radiative properties of these surfaces. Additionally, the reflectance, transmittance, and emittance of H_2O frost are of

Presented as Paper 71-447 at the AIAA 6th Thermophysics Conference, Tullahoma, Tenn., April 26-28, 1971, submitted December 30, 1970; revision received May 17, 1971. This research was sponsored by the Arnold Engineering Development Center, Air Force Systems Command, under Contract F40600-71-C-0002 with ARO, Inc.

Index Categories: Radiation and Radiative Heat Transfer; Thermal Surface Properties.

* Project Engineer, Aerospace Division, von Karman Gas Dynamics Facility. Associate Fellow AIAA.

† Supervisor, Research Section, Aerospace Division, von Kármán Gas Dynamics Facility; also Associate Professor of Aerospace Engineering, University of Tennessee Space Institute, Tullahoma, Tenn. Member AIAA.

‡ Research Assistant, von Karman Gas Dynamics Facility and University of Tennessee Space Institute, Tullahoma, Tenn.; presently Senior Engineer, Northrop Corporation, Huntsville, Ala. Member AIAA.

§ Research Physicist, Aerospace Division, von Kármán Gas Dynamics Facility; presently Research Assistant, Colorado State University, Fort Collins, Colo.

general interest with regard to calibration of low-temperature blackbodies.

Reflectance data reported heretofore on water cryodeposits, frost, and ice either have been specular reflectance measurements or relative reflectance measurements, or were reflection spectra that simply gave an indication of the presence of absorption bands without regard to the quantitative reflecting ability of the deposits. In addition, most of these measurements were for H_2O frosts formed at atmospheric pressure. Previously, the first two authors measured in situ the monochromatic angular-hemispherical reflectance of H_2O cryodeposits formed in vacuum¹ but these measurements were restricted to the wavelength range from 0.36 to 1.15 μ and were relative to the reflectance of MgO . Essentially nothing has been done to spectrally determine the absolute hemispherical-angular reflectance of H_2O frost or cryodeposits. The reasons for this are understandable and are due to the fact that: 1) the deposits often scatter a significant amount of radiation which means that either an integrating sphere or 2π steradian mirror must be used to sample or collect all the reflected energy, 2) studies of high-purity frosts require that the deposits be formed in vacuum, and 3) absolute spectral reflectance measurements, in general, require special care in the technique of measurement.

This investigation presents the absolute hemispherical-angular reflectance of H_2O cryodeposits for wavelengths from 0.5 to 12.0 μ . The deposits, up to 4.0 mm thick, were formed on LN_2 -cooled stainless steel surfaces that were either polished or coated with a black epoxy paint. An infrared integrating sphere discussed previously^{2,3} was used to make the absolute reflectance measurements. These data are presented as functions of substrate material, view angle, wavelength, and deposit thickness. The results show that H_2O deposit reflectances are strongly dependent on wavelength and on the manner in which the deposit is formed. Wherever possible, these results are discussed considering various optical applications of cryogenic surfaces. Since water vapor is the most abundant constituent of the Earth's atmosphere that will condense on LN_2 -cooled surfaces, the reflectances of these surfaces and H_2O frosts in general are of considerable interest.

Water Deposit Formation Properties

Ice formed at pressures of one atmosphere or less is designated as ice I and can have two crystalline forms, hexagonal (Ih) and cubic (Ic), and an amorphous form which has no crystalline structure. From the results summarized in Ref. 4, it would appear that water deposits formed from the vapor on surfaces in vacuum which are 115°K or colder will be amorphous. If the surface is between approximately 115°K and 150°K the deposit will be Ic. For surface temperatures higher than 150°K the frosts formed will be Ih. It is also generally agreed that these temperatures of formation are not rigid. Hence, mixtures of the different forms can be obtained in the vicinity of the stated temperatures.

The temperatures stated previously are those of the surface while the vapor is condensing. Once formed, the deposit can also change structure. The deposit can transform from amorphous to cubic to hexagonal but the processes are not reversible. The most conclusive method for studying these changes in crystalline form is through x-ray diffraction techniques such as used by Dowell and Rinfret.⁵ They found that if an H_2O deposit is warmed at a fairly high rate, i.e., 5°C/min, the amorphous to cubic transition would be observed in the vicinity of 145°K. This transition is an exothermic reaction in which there is a sudden increase in temperature from about 145°K up to approximately 165°K within seconds. Dowell and Rinfret also show that the conversion of amorphous to cubic can occur at lower temperatures but requires longer time periods. They also state

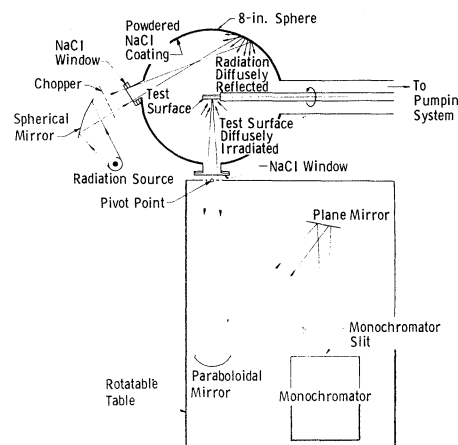


Fig. 1 Schematic of infrared integrating sphere.

that no further transformation change is seen until the temperature reaches 200°K whereupon Ic begins to transform to Ih. However, in Ref. 6 the Ic to Ih transition was reported to occur at about 170°K. Only relatively small heat releases have been observed during the cubic to hexagonal transformation.

Infrared absorption spectra of the two crystalline forms of ice I have been studied by Ockman,⁷ Bertie and Whalley,⁸ and Hornig, White and Reding.⁹ No significant differences were seen in the absorption spectra of the two forms. This means that the location of the major absorption bands occurs in the same vicinity for both Ih and Ic. Until the present study there have been no data available on the spectral infrared absorption of amorphous ice.

Apparatus

The infrared reflectometer system (see Fig. 1) has been previously discussed in Refs. 2 and 3. Absolute hemispherical-angular reflectance measurements were obtained in vacuum using a powdered sodium chloride coated integrating sphere. The test surface was one of the faces of a cryosurface and was either polished stainless steel or coated with black epoxy paint. A copper-constantan thermocouple was silver-soldered to the surface for monitoring the test surface temperature. To restrict the cryopumping area to only that of the cryosurface, the LN_2 supply lines inside the vacuum chamber were vacuum jacketed. A guard was attached at one end to the vacuum jacket with the other end closely surrounding, but not touching, the junction of the vacuum jacket with the cryosurface. By rotating the cryosurface, reflectance measurements could be made as a function of view angle from 0 to 60°, as measured from the test surface normal.

The optical transfer, source, and detection systems were the same as those described in Ref. 3. Radiation from a 1000-w tungsten-halogen lamp was chopped at 13 Hz and focused on the sphere wall (see Fig. 1). The radiation reflected from either the test surface or sphere wall was focused on the entrance slit of a single pass monochromator which had a NaCl prism as the dispersing element and a Reeder thermocouple as the detector.

A gas addition system was used to introduce H_2O vapor into the sphere to be cryopumped. Prior to flow of the H_2O vapor into the sphere, the distilled H_2O was further purified by boiling under vacuum and removing any desorbed gases with a mechanical pump. The mass flow rate of the water vapor through a rotameter was calibrated by weighing an evacuated glass flask, cooling it with LN_2 , and allowing the vapor to condense in the flask. After about 10 min of flow, the flask was again weighed on a balance which was accurate to better than 10^{-3} g. Knowing the total mass deposited

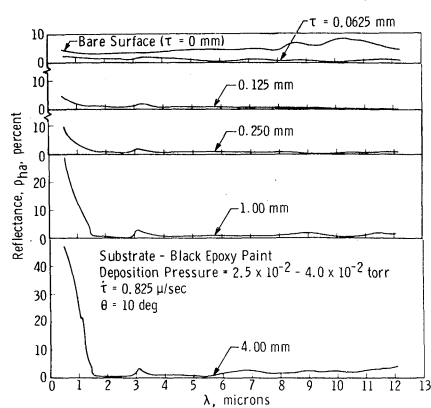


Fig. 2 Spectral reflectance of amorphous H_2O cryodeposits formed on a black epoxy paint substrate.

and the flow time, the mass flow rate was determined. This was found to be a very good calibration technique with reproducibility being within $\pm 1\%$. For all experiments reported herein a mass flow rate of $2.18 \times 10^{-3} \text{ g/sec}$ was used which yielded a mass deposition rate of $0.24 \text{ g/cm}^2 \cdot \text{hr}$.

Procedure

Prior to the cryodeposit reflectance measurements, the infrared integrating sphere was pumped down to approximately 5×10^{-7} torr and reflectance measurements were made on the warm bare test surface. These measurements were obtained using the hemispherical-angular technique described previously in Refs. 2 and 3. Briefly, radiation from an external source was focused on the NaCl -coated wall of the sphere after passing through a NaCl window. The radiation was diffusely reflected throughout the sphere resulting in the sphere wall being uniformly illuminated. This caused the test surface to be diffusely irradiated. The procedure was first to obtain a detector output $B_s(\theta, \lambda)$ by viewing the test surface at angle θ with respect to the surface normal. The wall of the sphere was viewed similarly for the same wavelength and another detector output $B_w(\lambda)$ recorded. Then the absolute reflectance was determined from $\rho_{\text{abs}}(\theta, \lambda) = B_s(\theta, \lambda)/B_w(\lambda)$. The important point for absolute reflectance measurements in the integrating sphere is that the area of the sphere wall viewed by the spectrometer is irradiated by the first reflection from the sphere wall whereas the test surface is not.

After the bare test surface reflectance was obtained, LN_2 was used to cool the cryosurface to an equilibrium temperature of 93°K . Upon valving off the integrating sphere from the pumping system, the H_2O vapor flow into the sphere was started. Because the gas was allowed to condense only on the cryosurface, a given flow time resulted in a certain deposit thickness τ . This could be calculated by knowing the mass deposition rate and density of deposit. The density of amorphous H_2O cryodeposits has been reported¹⁰ as 0.81 g/cm^3 . The deposits in this study were also amorphous and were formed under similar conditions to those stated in Ref. 10. Therefore, a density of 0.81 g/cm^3 was used in calculating all deposit thicknesses. In order to insure that these thicknesses were correct, deposits up to 130μ thick on stainless steel were checked optically by using thin film interference techniques with a He-Ne laser as a light source. The thicknesses determined by these two independent techniques were in good agreement, and indicated that the density used in the calculations was correct.

After each thickness of deposit had been formed, reflectance measurements were made as a function of wavelength from 0.5 to 12.0μ using the procedure discussed previously. Upon completion of reflectance measurements

for a given thickness, the flow of H_2O vapor was again started. The pressures during deposition remained relatively constant, ranging from 1×10^{-2} to 4×10^{-2} torr for the full range of thicknesses. This deposition pressure was an order of magnitude less than that for the H_2O deposits formed and measured in Ref. 1. The temperature of the test surface prior to any deposition was about 93°K . During the time of deposit formation, the temperature would rise about 2° to 3°K . For increasing deposit thickness, the temperature also gradually increased, with the final deposit thickness (4 mm) being formed at temperatures of approximately 103° to 106°K . As will be discussed later, this final temperature may have had some effect on the structure of the thick deposit.

Results

Amorphous Deposits on Black Epoxy Paint

The curve labeled $\tau = 0 \text{ mm}$ in Fig. 2 shows the reflectance of the black epoxy paint prior to cooldown. It is seen that this reflectance was 5% or less for wavelengths smaller than 8μ but increased to as high as 8–8.5% in the wavelength range between 8 and 12μ . Figure 2 also presents the reflectances of H_2O deposits on the black substrate for deposit thicknesses ranging from 0.063 mm up to 4.0 mm .¹¹ The pressure during deposition varied from 2.5×10^{-2} torr for the 0.063 mm -thick deposit to 4.0×10^{-2} torr for the 4.0 mm -thick deposit. The thickness deposition rate $\dot{\tau}$ of the H_2O deposits was constant at a value of $0.825 \mu/\text{sec}$.

It is seen in Fig. 2 that the reflectance of the 0.063 mm -thick deposit is less than that of the bare paint surface at all wavelengths. In the visible region the reflectance has been reduced from about 4.5% down to 2.0% and the reductions are even greater in the infrared ($\lambda > 1.0 \mu$). For the thicker H_2O deposits, the reflectance at the longer wavelengths remains essentially constant at thicknesses from 0.063 mm to 4.0 mm . In contrast, the data for a thickness of 4.0 mm shows the reflectance at 0.5μ to be about 47%. This increase in reflectance at the shorter wavelengths has a strong spectral dependence and, as shown in Refs. 12 and 13, is due to internal scattering. For the 1.0 mm -thick deposit the reflectance increases almost linearly with decreasing wavelength below about 1.5μ . To the eye, the thicker deposits (1.0 – 4.0 mm) had a slight milky-white translucent appearance, while deposits less than 0.25 mm thick could not be detected visually. In general, the deposits could be assumed to have an amorphous structure. This will be discussed in greater detail later.

For H_2O deposit thicknesses equal to or greater than 0.125 mm , a slight increase in reflectance in the wavelength region between 3.1 and 3.25μ can be seen. This increase is due to the anomalous dispersion effect which was observed earlier for CO_2 and discussed in Ref. 3. The reflectance peak is caused by the change in refractive index at an absorption band. Otherwise, in the infrared, the reflectance is essentially independent of thickness and wavelength for $\lambda > 1.5 \mu$. Even for the largest thickness, when the effects of internal scattering would be greatest, the reflectance is still well below that obtained for the bare substrate. In the infrared the general trend for water deposits formed on LN_2 -cooled substrates will be to make absorbing surfaces more absorbing.

The reflectance data reported in Fig. 2 were for a viewing angle θ of 10° . To determine the effect of varying θ , reflectance measurements were made at viewing angles from 0 to 60° and for wavelengths of 0.5 , 1.0 , 2.0 , 4.0 and 8.0μ . The data for $\lambda = 0.5$, 1.0 , and 2.0μ are shown in Fig. 3. There were no significant differences between the data for $\lambda = 2.0 \mu$ and that for $\lambda = 4.0$ and 8.0μ . As seen from the

¹¹ Additional experimental data are contained in Ref. 11.

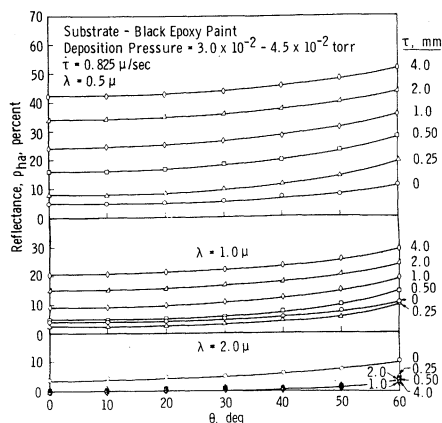


Fig. 3 Dependence of reflectance on view angle for amorphous H₂O deposits formed on a black epoxy paint substrate.

curves in Fig. 3, there were no major reflectance variations with view angle.

The change in H₂O reflectance with deposit thickness on a black paint substrate is shown in Fig. 4 for the wavelengths of 0.5, 1.0, 2.0, 4.0, and 8.0 μ. These data were obtained in an additional experiment as can be seen by the fact that the reflectance of the 4-mm-thick deposit in Fig. 4 for λ = 0.5 μ is 3 to 4% less than for the corresponding thickness and wavelength shown in Fig. 2. Figure 4 shows a gradual increase in reflectance with thickness for the 0.5- and 1.0-μ curves. For the other three wavelengths, the reflectance is largely independent (within 5%) of both thickness and wavelength.

The data shown in Fig. 4 were for deposits that were formed in layers rather than continuously. Figure 5 shows the variation of reflectance with thickness at a wavelength of 0.55 μ for an H₂O deposit formed continuously. Although there is only a slight change in the curve shape around 2.4 mm thickness, it is enough to indicate a possible structure change. At 2.0 mm thickness, the reflectance curve appears to have reached a plateau but then begins to rise again at a thickness of about 2.4 mm. The final reflectance of about 43% however, agrees with the 44% value at 0.55 μ for the 4-mm-thick deposit shown in Fig. 2. It is also near to the 43% value for the 0.5-μ curve shown in Fig. 4. Therefore, according to these results there are no significant differences in the reflectance of deposits formed continuously (Fig. 5) or in layers (Figs. 2 and 4).

In Ref. 3 an analytical model was presented for determining the reflectance of a uniform scattering and absorbing layer. To apply this model to the reflectance data shown in Fig. 4 for λ = 0.5 μ, the black paint surface having a refractive index¹³ $\bar{n} = 1.48 - i0.00$ was assumed to be diffusely reflecting** and the surface of the deposit, which has

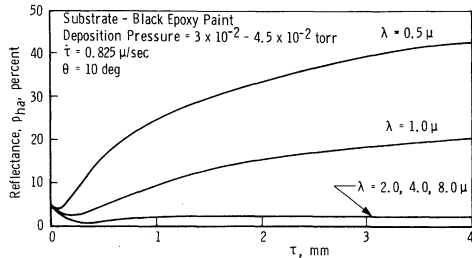


Fig. 4 Dependence of reflectance on thickness for amorphous H₂O deposits formed in layers on a black epoxy paint substrate.

** Reference 12 shows theoretically that the reflectance for a cryodeposit on a black substrate is independent of whether the substrate is assumed diffuse or specular.

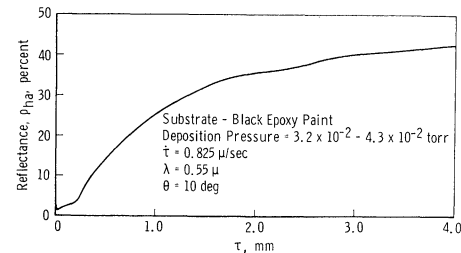


Fig. 5 Dependence of reflectance on thickness for an amorphous H₂O deposit formed continuously on a black epoxy paint substrate, λ = 0.55 μ.

a refractive index¹⁰ $n = 1.266$ was assumed to be specular. With these assumptions the model was first used to determine^{3,12} the scattering (σ) and absorption (k) coefficients from the reflectance data for the two deposit thicknesses indicated in Fig. 6 (see arrows). For these thicknesses, 0.5 and 1.0 mm, thin-film interference effects need not be considered. The value for σ was 12.48 cm⁻¹ and for k , 0.984 cm⁻¹. Since the deposits were predominantly amorphous, or glasslike, the scattering coefficient, as expected, was considerably lower than that for most H₂O frost. It is important to point out that the scattering and absorption coefficients determined are valid only for this one deposit. This is due to the many factors which can influence the formations of H₂O deposits as mentioned earlier. After σ and k were determined, they were used to calculate the reflectance for each deposit thickness listed in the table of Fig. 6. The analytical and experimental results are compared in Fig. 6 and agreement is good for deposits 2 mm thick and less. For the 4.0-mm deposit the reflectance determined experimentally is about 5% higher than the analytical prediction. The good agreement for the smaller thicknesses indicates that the deposit is homogeneous, and the disagreement for the largest thickness suggests that the outer layer of the 4-mm-thick deposit was slightly more reflecting than the inner 2 mm. It is speculated that the outer layer was more reflecting as a result of being partially Ic. From the reflectance vs thickness curve shown in Fig. 5 this would seem very likely. Since the thick deposits did appear somewhat white, they were presumably at least partially cubic crystalline. The only other possible explanation for this appearance would be the presence of voids throughout the deposit which would serve as scattering centers.

Crystalline Deposits on Black Epoxy Paint

After the reflectance measurements were completed for the deposits in Fig. 2, the LN₂ flow was turned off and the test surface allowed to warm up. As it warmed, both the cryosurface temperature and the reflectance at a wavelength of 0.55 μ were monitored. These data are shown in Fig. 7. The heat load from the radiation source caused the cryo-

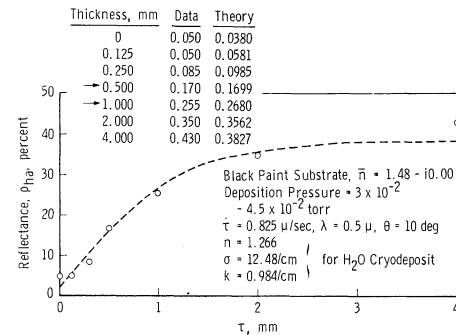


Fig. 6 Comparison of experimental and analytical results for reflectance of amorphous H₂O deposits formed on a black epoxy paint substrate.

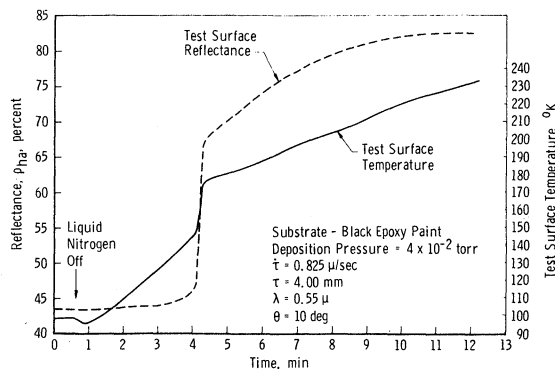


Fig. 7 Reflectance and temperature variation of H_2O cryodeposit during structural change from amorphous to Ic to Ih .

surface to warm up at a fairly high rate of about $15^\circ\text{K}/\text{min}$. As can be seen in Fig. 7, the reflectance stayed constant until a temperature of about 145°K was reached. At this instant, there was a rapid increase in both the reflectance and temperature of the H_2O deposit which is characteristic of transformations from the amorphous to cubic structure. Further warming caused a steady rise in reflectance and temperature until at 233°K the reflectance leveled off at a value of 83%. After the test surface reached 233°K the surface was again cooled with LN_2 to approximately 100°K , and the spectral reflectance measured from 0.5 to $12.0\ \mu$. The resulting reflectance, shown in Fig. 8, is greater by a factor of about 2 over that observed for the deposit before warmup. Increased internal scattering by the H_2O deposit accentuates the absorption bands at 1.04 , 1.25 , 1.55 , 2.03 , and in the vicinity of 2.85 – $3.25\ \mu$. Substantial internal scattering is also seen for the longer wavelengths up to $12.0\ \mu$.

After the spectral reflectance measurements shown in Fig. 8 were completed, the test surface was again allowed to warm up. However, no abrupt changes in temperature or reflectance were observed. Therefore, the structural changes are irreversible, at least for periods of a few hours. The change in reflectance is caused by the change of the deposit, originally in a predominantly amorphous state, to the cubic crystalline state. This is an exothermic process as indicated by the sudden jump in temperature at 145°K in Fig. 7. After warmup to 233°K the final state is undoubtedly hexagonal. The gradual increase in reflectance seen in Fig. 7 for temperatures beyond 175°K is due to the relatively slow conversion of the cubic form to hexagonal.

Amorphous Deposits on Stainless Steel

To study the dependence of cryodeposit reflectance on substrate reflectance, H_2O deposits were formed on the LN_2 -cooled polished stainless steel surface. This was the same test surface used previously but with the paint removed and the surface repolished. The reflectance of the bare surface ($\tau = 0\ \text{mm}$) prior to cooldown is shown in Fig. 9. For the thinnest deposit studied, $30\ \mu$, the reflectance was reduced significantly. Absorption bands can be seen to occur at $1.55\ \mu$ and $2.0\ \mu$, around $3.0\ \mu$, and at $4.5\ \mu$. For wavelengths between 5.5 and $12\ \mu$ the deposit absorbs strongly for all wavelengths but does show slight reflectance peaks in the vicinity of 8.0 , 8.75 and $9.6\ \mu$. Regions of maximum transmission through the deposit are seen to be at about 3.70 and $5.1\ \mu$ and for most wavelengths below $2.5\ \mu$. The peak at $3.7\ \mu$ also corresponds to a transmission window in the gaseous phase of water. For thicker deposits in Fig. 9, the peak at $3.7\ \mu$ disappears and the reflectance decreases for all wavelengths. The edge of strongest absorption moves from $3.0\ \mu$ for $\tau = 0.125\ \text{mm}$ to $1.5\ \mu$ for $\tau = 4.00\ \text{mm}$. In the visible and near infrared the reflectance drops to about 30% for the $0.125\ \text{mm}$ thick deposit. At this thickness the sur-

face appears tannish-brown in color. Further increase in deposit thickness causes the visible and near infrared reflectance to increase. Finally, for a deposit thickness of $4.0\ \text{mm}$, the reflectance spectrum in Fig. 9 looks very similar to that for the 4.0-mm-thick deposit on the black substrate (Fig. 2). The main difference is that the reflectance in the infrared appears to be about 5% higher for the deposits formed on the stainless steel substrate.

The reflectance variation with H_2O deposit thickness on a stainless steel substrate is shown in Fig. 10 for wavelengths of 0.5 , 1.01 , 2.02 , 4.10 and $8.05\ \mu$. These data are for the deposits whose spectral reflectances are shown in Fig. 9. The reflectance at $1.5\ \mu$ drops from an initial value of 50% down to 30% and then is followed by a gradual rise back up to 46% at 4.0-mm thickness. This is almost back up to the initial value. For the other wavelengths, the reflectance is considerably less than the initial value regardless of the deposit thickness. The behavior of the $0.5\text{-}\mu$ curve has been explained earlier for CO_2 in Ref. 3. It was determined that the initial drop in reflectance is due to two causes: 1) the change in the relative refractive index at the stainless steel substrate, and 2) a further decrease caused by trapping of radiation in the deposit because of the critical angle effect. The second decrease is a result of scattering of radiation such that the rays are internally incident on the deposit surface at angles greater than the critical angle. This radiation is then totally reflected back to the substrate which increases the possibility of its absorption by the stainless steel.

Crystalline Deposits on Stainless Steel

After the reflectance measurements for the $4.00\ \text{mm}$ deposit in Fig. 9 had been completed, the chamber was brought up to $740\ \text{mm}$ pressure with dry nitrogen while the reflectance at $0.55\ \mu$ was monitored. Although the LN_2 flow through the test surface was continued, the temperature increased from about 100°K to 115°K . During this pressurization there also was a gradual increase in deposit reflectance from the initial value of 46%. After an hour the reflectance had risen to about 65%. This increase was probably caused by the surrounding gas warming the outer portion of the deposit. The test surface temperature was 115°K which was considerably less than the transition temperature of 145°K observed earlier. However, because of the high heat load from the light source the outer portion of the H_2O frost may have reached sufficiently high temperatures to cause the phase transition from the amorphous to cubic state. The transition would begin on the outer surface and advance slowly inward with time. Dowell and Rinfret⁵ have shown that amorphous ice will change to cubic for temperatures between 113° and 145°K with the deposits at the colder temperatures requiring much longer times to transform. When

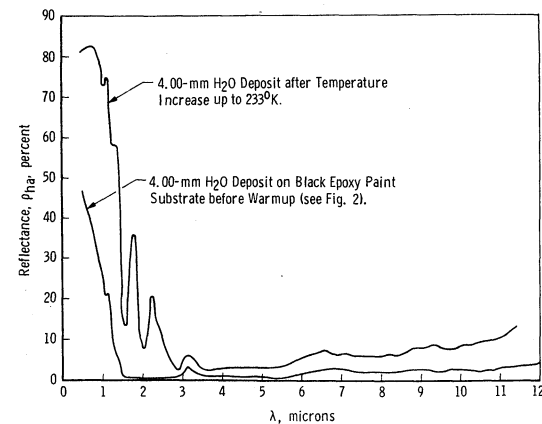


Fig. 8 Comparison of reflectances of a 4-mm H_2O deposit on black epoxy paint before warmup (amorphous structure) and after warmup (hexagonal structure).

the deposit reflectance had reached 65% the chamber was evacuated to approximately 10^{-5} torr and the LN_2 turned off to allow the cryosurface to warm. As the temperature reached $145^\circ K$ there was again a sudden increase in both temperature and deposit reflectance but the sudden reflectance increase was only about 6%. This was considerably less than the jump observed in Fig. 7. After the sudden reflectance increase, the reflectance continued to increase gradually up to about 83% in the same manner as shown for the deposit in Fig. 7. The small jump was due to the fact that most of the amorphous ice had already transformed to the cubic state.

Figure 11 shows the spectral reflectance of the 4-mm H_2O deposit on stainless steel after the system had been pressurized, the chamber again evacuated, and the cryosurface temperature raised to $200^\circ K$ and then lowered to $100^\circ K$. The shape and magnitude of this reflectance curve resembles that of the analogous curve in Fig. 8 with some slight differences. For both cases, absorption bands appear at 1.04, 1.25, 1.55, 2.04 and around 3.0μ . In Fig. 11 there is a peak in the reflectance at about 3.5μ whereas no peak was observed for the annealed deposit on the black substrate (Fig. 8). The main difference between the two experiments was the fact that the annealed deposit reflectance shown in Fig. 11 was obtained after the deposit had been exposed to a dry N_2 pressure of 740 mm. Undoubtedly, N_2 gas was absorbed by the deposit. Since no significant difference is seen between the reflectances of the two annealed deposits for wavelengths slightly less or greater than 3.5μ , it would appear that the reflectance peak at 3.5μ is not due to scattering alone but is caused mostly by increased transmission. A similar peak is present in reflectance data obtained by other investigators for H_2O frosts formed at atmospheric pressure^{14,15} and has also been observed in this laboratory when the frost was pumped directly from the atmosphere.

Discussion

As indicated by the results shown in Figs. 2-11, H_2O deposits may have an appreciable effect on the thermal radiative properties of surfaces employed in cryogenic applications. For example, the infrared reflectance of a black painted surface can be reduced to 1% or less which obviously

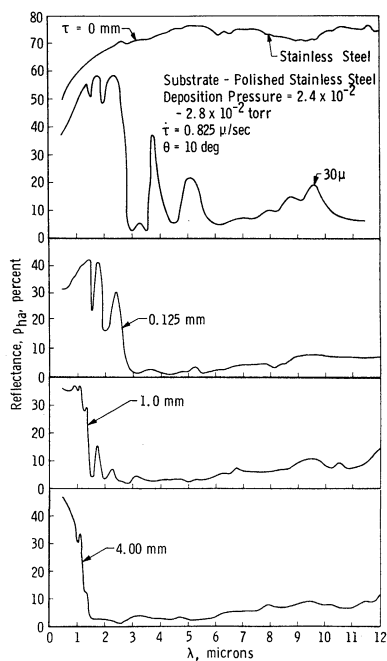


Fig. 9 Spectral reflectance of amorphous H_2O cryodeposits formed on a polished stainless steel substrate.

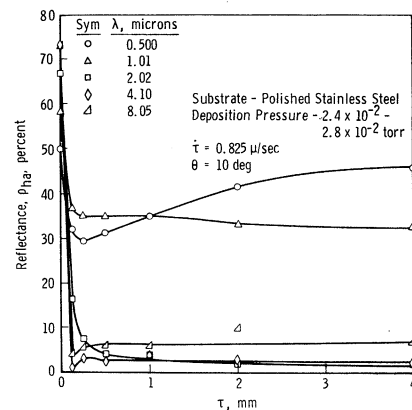


Fig. 10 Dependence of reflectance on thickness for amorphous H_2O cryodeposits formed on a polished stainless steel substrate.

is an important factor in certain space simulation experiments where background infrared radiation must be minimized. In such studies the surroundings are black cryogenically cooled walls. By precoating the cold walls with a thin H_2O deposit 50-100 μ thick, reflectances of 1% or less could be easily achieved provided that the deposit formed was amorphous. The vapor pressure of water deposits formed at these temperatures ($77^\circ-4^\circ K$) is so low (less than 10^{-24} torr) that migration to other cooled optical surfaces within the chamber would not be a problem. For space simulation chambers in general, H_2O can deposit in any of the 3 different forms, Ih, Ic, or amorphous. Which of these 3 types or what mixtures of these forms occur during deposition will be determined by the cold wall temperature. Although the infrared reflectance of a black surface could be greatly reduced by a thin layer of amorphous ice, a crystalline layer of the same thickness could cause an increase in the visible and near infrared reflectance. This increase could be an order of magnitude if the deposit formed was ice Ih. Therefore, care must be taken to maintain the cold wall at a temperature less than approximately $100^\circ K$. Also, a "hot spot" on a cryogenically cooled panel could cause the surface reflectance to increase since the formation of ice Ih or Ic at a local point can propagate across an amorphous deposit.

The effect of water deposits formed on polished stainless steel indicates that the presence of even very thin films of H_2O on a cooled mirror can change the infrared reflective properties from highly reflecting to highly absorbing. This reduction in reflectance can be especially crucial in airborne applications of cooled optics where contamination by thin water films will be inevitable. Additionally, the highly absorbing feature of water deposits for wavelengths greater

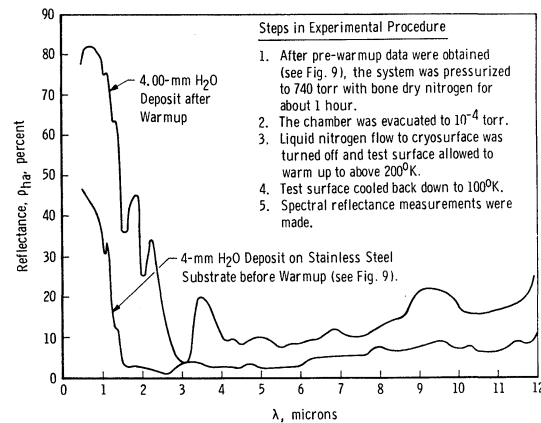


Fig. 11 Comparison of reflectances of a 4-mm H_2O deposit on stainless steel before warmup (amorphous structure) and after warmup (hexagonal structure).

than about 1.5μ will make the deposits even more troublesome in the infrared region as was shown by a deposit only 30μ thick on the polished stainless steel surface (Fig. 9). For any system requiring cooled optics a concerted effort will be necessary to minimize the contamination of the optical surfaces by H_2O .

Previously, the phase changes of H_2O have been studied using calorimetric techniques and x-ray diffraction. The results shown in Fig. 7 are unique in that they show quantitatively the visual ($\lambda = 0.55 \mu$) changes in reflectance during these phase changes. In Fig. 7 the reflectance change was from about 43% up to 66% which was easily observed visually. The amorphous to Ic transition would start at some point on the test surface and spread over the remainder of the surface within 10-15 sec. In contrast, the transition from cubic to hexagonal was gradual, and the appearance of the deposit after it had transformed to hexagonal was much whiter than that for the cubic structure.

Although the absorption bands seen in Figs. 2, 8, 9 and 11 were found to occur at the same wavelength for the different structural forms of H_2O deposit, this was not unexpected. It has been pointed out previously⁸ that the major absorption bands for the hexagonal and cubic form of H_2O occur at approximately the same wavelengths. From the present study it is seen that this conclusion can also be extended to include amorphous ice.

Conclusion

The present investigation has presented in situ hemispherical-angular reflectance measurements of H_2O deposits formed on LN_2 -cooled surfaces in vacua. Deposits from 0.03 to 4.0 mm thick were studied and found to appreciably affect the absolute reflectance over the entire wavelength range covered, 0.5 to 12.0μ . From the results of this study, the following observations are made:

1) The reflectances of cold black surfaces can be reduced by coating them with a thin solid film of H_2O . In particular, between wavelengths of 2 and 12μ , the reflectance can be reduced to 1% or less for an H_2O deposit thickness of 50-100 μ .

2) H_2O deposits formed on a polished stainless steel surface reduce the reflectance over the entire wavelength range. In the infrared a deposit only 30μ thick reduces the reflectance from about 75% down to about 15%. This indicates that thin H_2O films can seriously affect the infrared performance of cooled optics.

3) The reflectance of an H_2O cryodeposit is extremely sensitive to the temperature of the deposit or of the surface on which the deposit is formed. All three structural forms of ice I are observed, amorphous, cubic (Ic), and hexagonal (Ih). The exothermic transition from the amorphous to cubic state occurs at about 145°K . Further temperature increase causes the deposit to transform to the hexagonal configuration. The reflectance of these deposits increases as the deposit changes from amorphous to Ic to Ih .

4) Weak absorption bands occur at wavelengths of 1.04 and 1.25μ and strong bands at 1.55 , 2.04 , 3.0 and 4.5μ . A broad region of strong absorption is observed for wavelengths between 3 and 12μ . The wavelength region of strongest absorption appears to be between 3 and 7μ . All absorption

bands occur at the same wavelengths for Ih and amorphous ice.

5) In the reflectance of H_2O on black paint, a small anomalous dispersion peak is observed at wavelengths between 3.1 and 3.25μ .

6) After a 4 mm H_2O deposit, formed in vacuo on stainless steel, is exposed to dry nitrogen gas at 740 torr pressure, a peak appears in the spectral reflectance at a wavelength of 3.5 - 3.7μ .

References

- 1 Wood, B. E. and Smith, A. M., "Spectral Reflectance of Water and Carbon Dioxide Cryodeposits from 0.36 to 1.15μ ," *AIAA Journal*, Vol. 6, No. 7, July 1968, pp. 1362-1367.
- 2 McCullough, B. A., Wood, B. E., Smith, A. M., and Birkebak, R. C., "A Vacuum Integrating Sphere for In Situ Reflectance Measurements at 77°K from 0.5 to 10μ ," *Progress in Astronautics and Aeronautics, Thermophysics of Spacecraft and Planetary Bodies*, Vol. 20, Academic Press, New York, 1967, pp. 137-150.
- 3 Wood, B. E., Smith, A. M., Roux, J. A., and Seiber, B. A., "Spectral Absolute Reflectance of CO_2 Frosts from 0.5 to 12.0μ ," *AIAA Journal*, Vol. 9, No. 7, July 1971, pp. 1338-1344.
- 4 Sugisaki, M., Suga, H., and Seki, S., "Calorimetric Study of Glass Transition of the Amorphous Ice and of the Phase Transformation Between the Cubic and the Hexagonal Ices," *Physics of Ice*, Plenum Press, 1969, p. 329.
- 5 Dowell, L. G., and Rinfret, A. P., "Low Temperature Forms of Ice as Studied by X-Ray diffraction," *Nature*, Vol. 188, Dec. 31, 1960, pp. 1144-1148.
- 6 Bertie, J. E., Calvert, L. D., and Whalley, E., "Transformations of Ice II, Ice III and Ice V at Atmospheric Pressure," *The Journal of Chemical Physics*, Vol. 38, No. 4, 1963, pp. 840-846.
- 7 Ockman, N., "The Infrared and Raman Spectra of Ice," *Advances in Physics*, Vol. 7, 1958, pp. 199-220.
- 8 Bertie, J. E. and Whalley, E., "Infrared Spectra of Ices Ih and Ic in the Range 4000 to 350 cm^{-1} ," *The Journal of Chemical Physics*, Vol. 40, No. 6, 1964, pp. 1637-1645.
- 9 Hornig, D. F., White, H. F., and Reding, F. P., "The Infrared Spectra of Crystalline H_2O , D_2O , and HDO ," *Spectrochimica Acta*, Vol. 12, 1958, pp. 338-349.
- 10 Seiber, B. A., Wood, B. E., Smith, A. M., and Müller, P. R., "Density of Low Temperature Ice," *Science*, Vol. 170, No. 3958, Nov. 6, 1970, pp. 652-654.
- 11 Wood, B. E., Smith, A. M., Seiber, B. A., and Roux, J. A., "Infrared Reflectance of Water Frosts Condensed on Liquid-Nitrogen-Cooled Surfaces in Vacuum," AEDC-TR-70-215 (AD715915), Dec. 1970, Arnold Engineering Development Center, Arnold Air Force Station, Tenn.
- 12 Roux, J. A., "Radiative Heat Transfer of Coatings on a Cryogenic Surface," Ph.D. dissertation, Department of Mechanical Engineering, Dec. 1970, University of Tennessee, Knoxville, Tenn.
- 13 Müller, P. R., "Measurements of Refractive Index, Density, and Reflected Light Distributions for Carbon Dioxide and Water Cryodeposits and also Roughened Glass Surfaces," Ph.D. dissertation, Department of Mechanical Engineering, 1969, University of Tennessee, Knoxville, Tenn.
- 14 Zander, R., "Spectral Scattering Properties of Ice Clouds and Hoarfrost," *Journal of Geophysical Research*, Vol. 71, No. 2, 1966, pp. 375-378.
- 15 Keegan, H. J., and Weidner, V. R., "Infrared Spectral Reflectance of Frost," *Journal of the Optical Society of America*, Vol. 56, No. 4, 1966, pp. 523-524.